Improved model for predicting the hydraulic conductivity of soils based on the Kozeny–Carman equation

Mengting Wang, Jianjun Wang, Guangli Xu, Yuhao Zheng and Xuan Kang

ABSTRACT

The saturated hydraulic conductivity of soils is a critical concept employed in basic calculation in the geotechnical engineering field. The Kozeny–Carman equation, as a well-known relationship between hydraulic conductivity and the properties of soils, is considered to apply to sands but not to clays. To solve this problem, a new formula was established based on Hagen–Poiseuille's law. To explain the influence on the seepage channel surface caused by the interaction of soil particles and partially viscous fluid, the surface area ratio was introduced. A modified framework for determining the hydraulic radius was also proposed. Next, the relationship between the effective void ratio and the total void ratio was established for deriving the correlation of hydraulic conductivity and total void ratio. The improved equation was validated using abundant experimental results from clays, silts, and sands. According to the results, the accuracies of the proposed model with two fitted multipliers for clays, silts, and sands are 94.6, 96.6, and 100%, respectively, but with only one fitted parameter, the accuracies are 97.1, 91.5, and 100%, respectively. The proposed model can be considered to have a satisfactory capability to predict hydraulic conductivity for a wide variety of soils, ranging from clays to sands.

Key words | effective void ratio, hydraulic conductivity, hydraulic radius, soils, specific surface, surface area ratio

Mengting Wang
Jianjun Wang
Guangli Xu (corresponding author)
Yuhao Zheng
Xuan Kang
Faculty of Engineering,
China University of Geosciences,
Wu Han 430074,
China
E-mail: xu1963@cug.edu.cn

Jianjun Wang
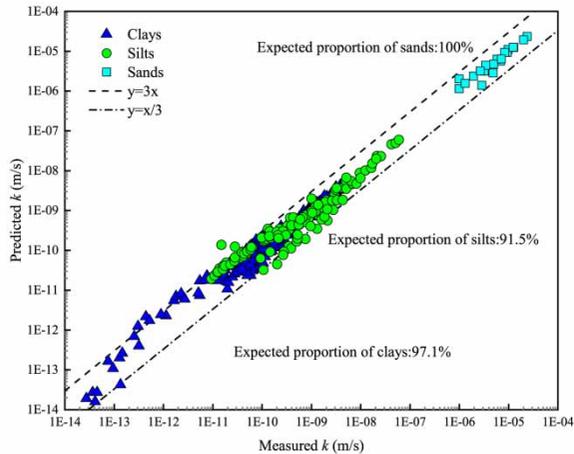CCCC Highway Consultants Co., Ltd,
Beijing 100088,
China

Xuan Kang
Institut für Geotechnik,
Universität für Bodenkultur,
Feistmantelstrasse 4, A-1180 Vienna,
Austria

HIGHLIGHTS

- An improved model of the soil particle-water system was proposed.
- The surface area ratio δ is introduced.
- We establish an improved method for estimating the effective void ratio.
- The relationship between LL and As for clay was established.
- The correlation between the parameters C and the specific surface area of soils was established.
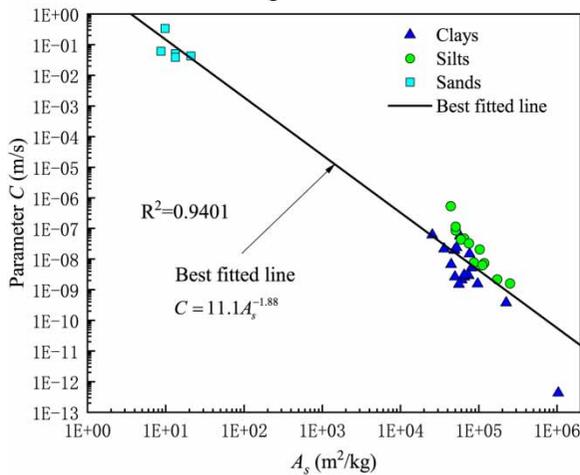
GRAPHICAL ABSTRACT

Predicted k versus measured k values for different soils

Relationship between C and As

INTRODUCTION

Saturated hydraulic conductivity represents the ability of soils to transmit water under saturated conditions (Jabro 1992) and is also related to the characteristics of both fluid and its transport medium (Najafzadeh *et al.* 2017). When resolving some geotechnical engineering problems, such as the settlement of saturated soils, slope stability, and design of earth dams (Onur & Shakoor 2015), a reliable value of the hydraulic conductivity is required. Similarly, the determination of saturated hydraulic conductivity plays a key role in the drinking water supply, the management of

water resources, water contamination, and facilities engineered for waste storage (Chapuis 2012).

However, the hydraulic conductivity value of soils is generally difficult to determine since it depends on numerous parameters, i.e., particle size distribution, particle shape, porosity, void ratio, saturation, clay content, and Atterberg Limit (Mesri & Olson 1971a, 1971b; Tan 1989; Alyamani & Sen 1993; Benson & Trast 1995; Chapuis & Aubertin 2003; Chapuis 2004; Trani & Indraratna 2010; Urumović & Urumović 2016; Kango *et al.* 2019). In addition,

it would be more useful to characterize the diameters of pores, rather than those of the grains, in hydromechanics (Salarashayeri & Siosemarde 2012). Hence, some researchers have studied the pore geometry about the control permeability of porous media, including pore size distribution, tortuousness of capillaries, the coordination number of the pore, and pore shape (Fauzi 2002; Xu & Yu 2008; Xiao et al. 2019).

Generally, the saturated hydraulic conductivity value of soils can be measured by both field and laboratory tests or predicted. In real situations, accurate estimates of hydraulic conductivity in the field are limited to the deficient comprehension of the aquifer geometry and hydraulic boundaries (Uma et al. 1989), and the cost of the field tests is quite high. However, the samples used in laboratory tests cannot be totally representative in most cases, and the time limitation also makes laboratory tests defective, as well (Boadu 2000).

Due to the diversity and complexity of the factors influencing hydraulic conductivity, numerous investigators have studied the empirical or semi-empirical formulas for hydraulic conductivity. The Hazen formula proposed by Hazen (1892) and the Kozeny–Carman equation proposed by Kozeny (1927) and then modified by Carman (1937) are used most often. Hazen proposed a formula to determine saturated hydraulic conductivity of sandy soils:

$$k = C_H D_{10}^2, \tag{1}$$

where k is the hydraulic conductivity (cm/s), C_H is the Hazen empirical coefficient, and D_{10} is the particle size for which 10% of the soil is finer (mm).

The Hazen formula was originally developed for the determination of hydraulic conductivity of uniformly graded sand but is also useful for the fine sand to gravel range, provided that the sediment has a uniformity coefficient less than 5 and an effective grain size between 0.1 and 3 mm (Odong 2007). The published value of C_H varies from 1 to 1,000. A change of three orders of magnitude makes the prediction result inevitably produce a certain deviation due to the difficulty of including all possible variables in porous media by effective diameter D_{10}. The formula has continued to be used for its simplicity and ease of memorization (Carrier 2003).

The Kozeny–Carman equation was proposed by Kozeny and improved by Carman:

$$k = C \frac{g}{\mu_w \rho_w} \frac{e^3}{S_S^2 G_s^2 (1+e)}, \tag{2}$$

where k is the hydraulic conductivity (cm/s), C is a constant related to the shape and tortuosity of channels (Hansen 2004), with a value approximately 0.2 (Taylor 1948), g is the gravitational constant (m/s²), ρ_w is the density of water (kg/m³), ρ_s is the density of solids (kg/m³), G_s is the specific gravity of solids ($G_s = \rho_s/\rho_w$), μ_w is the dynamic viscosity of water (N·s/m²), S_S is the specific surface (m²/kg), and e is the void ratio.

The Kozeny–Carman equation is considered to predict hydraulic conductivity of sandy soils but cannot be applied to the prediction of clayey soils (Lambe & Whitman 1969) without considering the electrochemical reactions between the soil particles and water (Carrier 2003). Some investigators have also validated the Kozeny–Carman equation in clay. The results show that the Kozeny–Carman equation can obtain ideal calculation results for sandy soil and silty clay. However, when calculating the hydraulic conductivity of clay, the predicted value of the Kozeny–Carman equation differs greatly from the experimental value.

Taylor (1948) proposed that a thin surface film of water was bound to all clay particles. Because of the bound water, seepage occurs only through a part of the pore space. Therefore, an improved concept of void ratio should be established to extend the use of the equation.

Saturated clays contain free water in addition to strongly adsorbed water (Dolinar et al. 2007). For clayey soils, only the part of pores occupied by free water affects the hydraulic conductivity or is effective. Therefore, the essential use of the Kozeny–Carman equation to predict the hydraulic conductivity of fine-grained soils is to propose a method to estimate an effective void ratio.

At present, there is little research work for the specific surface area correction of the Kozeny–Carman equation. In past research, the surface area loss due to the contact of soil particles was usually ignored when deducing the equation of the soil hydraulic conductivity, and the reduction in the surface area of the seepage pipes caused by contacts

between particles was also not considered. Thus, it cannot really reflect the pore structure characteristics of clay.

To modify the Kozeny–Carman equation to predict hydraulic conductivity for a wide range of soils and enhance its accuracy, a surface area ratio δ is introduced in this paper to obtain the reduced surface area accurately, which enhances the calculation accuracy of the Kozeny–Carman equation. We also establish an improved method for estimating the effective void ratio. The performance and applicability of the improved equation are validated with experimental data for clays, silts, and sands.

EFFECTIVE VOID RATIO

The void ratio, a dominant parameter for soils, can be divided into effective void ratio and ineffective void ratio in soil. The effective void ratio contributes mainly to seepage, while ineffective void ratio has little influence on seepage. The ineffective void ratio consists mainly of unconnected pores, dead-end pores, and pores occupied by the bound water adsorbed to the surfaces. The quantity of immobile water depends on many factors such as the mineral composition and the physicochemical properties of the soils (specific surface and cation exchange capacity), geometric characteristics of the pores and particles, salinity of the flow, and temperatures of the pore water (Koponen *et al.* 1997; Ren *et al.* 2016; Dolinar & Trcek 2019). Therefore, all ineffective pores of clay can be considered to be occupied by the bound water adsorbed to the surfaces.

According to the above, there is mobile water that can flow freely and immobile water that cannot flow freely in the soils (Figure 1). Then, for a saturated soil, the effective porosity n_e is defined as the ratio of the pore volume occupied by the mobile water to the total pore volume (Ahuja *et al.* 1984). The effective void ratio e_e and the ineffective void ratio e_i are the ratio of mobile water volume and immobile water volume to the solid volume, respectively.

$$e_e = \frac{V_{mw}}{V_s}, \tag{3}$$
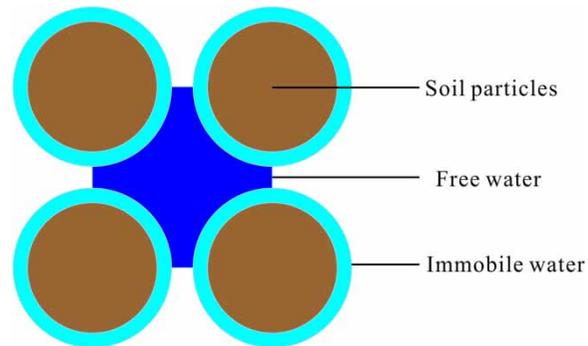
$$e_i = \frac{V_{iw}}{V_s}, \tag{4}$$

Figure 1 | Distribution of the pore water.

where V_{mw} is mobile water volume, V_{iw} is immobile water volume, and V_s is solid volume.

Figure 1 shows a commonly used model of pore water distribution. Head losses occur when the flow of water through seepage pipes of soils is due to the friction between soil particles and water and the friction inside the fluid. In a fluid undergoing laminar flow, variations in velocity from point to point are accompanied by friction losses. The surface of seepage pipes is composed of the surface of the soil particles. The surface area of the voids is usually considered equal to the surface area of the particles based on the assumption that the amount of surface area lost to the contacts between particles is negligibly small. However, the area lost to the contacts between particles cannot be ignored because of differences in the shape and size of soil particles, resulting in a corresponding reduction in the surface area of the seepage pipes (Figure 2).

Water flows around the soil particles in the pores but has difficulty flowing through the narrow space caused by
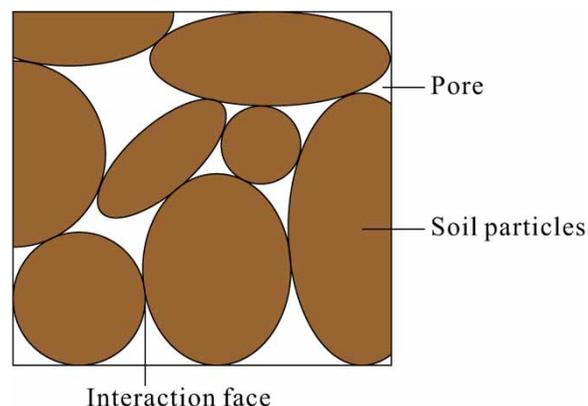

Figure 2 | Contact of the soil particles.

the contacts between particles. Therefore, this part of the surface area has no actual effect on seepage. Poiseuille's law proposed that the velocity at any point in the round capillary tube (Figure 3) can be described as follows:

$$v = \frac{\gamma_w i}{4\mu}(R^2 - r^2), \tag{5}$$

where R is the radius of a capillary tube, r is the radius of any concentric cylinder of liquid within the tube, γ_w is the unit weight of water, i is the hydraulic gradient, μ is the dynamic viscosity of water, and v is the velocity of a fluid at a distance r from the centre of the capillary tube. In laminar flow, the fluid in contact with the inside surface of the pipe ($r = R$) has been shown to have zero velocity, which means that there is a part of the viscous water occupying the corresponding surface area of the soil particles. This part of the surface area also has no contribution to the head losses of the fluid. A surface area ratio δ is introduced, then given by

$$S_s = \delta S_D, \tag{6}$$

where S_s is the surface area of all soil particles, and S_D is the reduced surface area.

Following the above analysis, an improved model has been established (Figure 4). If the immobile water can be regarded as part of the solid soil, then a new equivalent soil particle consisting of the soil particle and immobile water is proposed. The surface area is lost due to the contacts between new equivalent particles. A part of the thin viscous water is adsorbed on the surface, which is considered to play a role in reducing surface area only without counting as immobile water.
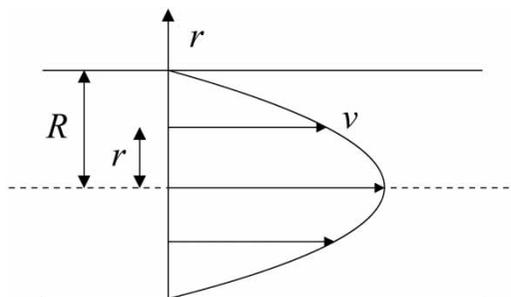
Figure 3 │ Velocity distribution in a round capillary tube.
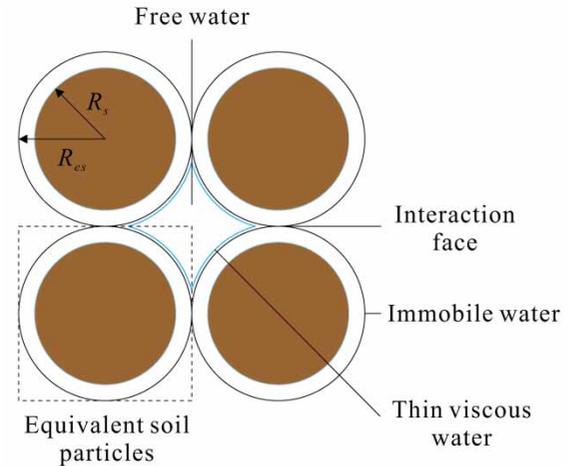
Figure 4 │ Improved model of the soil particle-water system.

The expression for flow through a circular tube is given by Taylor (1948):

$$Q = \frac{1}{2}\frac{\gamma_w R_H^2}{\mu} ia, \tag{7}$$

We can conclude that the flow through any given geometrical shape of cross-section is given by

$$Q = C_s \frac{\gamma_w R_H^2}{\mu} ia, \tag{8}$$

where C_s is a shape constant that has a definite value for any specific shape of the cross-section. The shape constant can be evaluated mathematically for a simple shape. a is the area of the effective tube and R_H is the hydraulic radius, which is defined as the ratio of the area of the cross-section available for flow S_w to the wetted perimeter P_w,

$$R_H = \frac{S_w}{P_w} \tag{9}$$

For a cross-section of a soil, the area of the effective tube a is equal to the area of the mobile water. The total area of the cross-section is S_t, the effective porosity is n_e. Then

$$n_e = \frac{V_{mw}}{V_s + V_{mw} + V_{iw}} = \frac{e_e}{1+e}, \tag{10}$$

$$a = S_t n_e = S_t \frac{e_e}{1+e}, \tag{11}$$

Substitution of Equation (11) into Equation (8) gives

$$Q = C_s \frac{\gamma_w R_H^2}{\mu} \frac{e_e}{1+e} i S_t, \tag{12}$$

According to Darcy's law,

$$Q = k_{sat} i S_t, \tag{13}$$

Combining Equations (12) and (13) gives

$$k_{sat} = C_s \frac{\gamma_w R_H^2}{\mu} \frac{e_e}{1+e}, \tag{14}$$

If the length of the tube is designated L, then the hydraulic radius R_H can be expressed as

$$R_H = \frac{S_w}{P_w} = \frac{S_w L}{P_w L} = \frac{V_w}{S_{wl}}, \tag{15}$$

where V_w is the volume of flow tubes and S_{wl} is the surface of flow tubes. S_{wl} can be expressed as

$$S_{wl} = S_{es}/\delta, \tag{16}$$

where δ is the surface area ratio and S_{es} is the surface area of new equivalent soil particles. If the soil consists of homogeneous spherical particles with a radius of R_s, then the new equivalent soil particles have a radius of R_{es}.

The volume of the new equivalent soil particle can be written as

$$V_{es} = e_i V_s + V_s = (1 + e_i) V_s \tag{17}$$

Then, the R_{es} can be expressed as

$$\frac{V_{es}}{V_s} = \frac{\frac{4}{3}\pi R_{es}^3}{\frac{4}{3}\pi R_s^3} = \frac{R_{es}^3}{R_s^3} = 1 + e_i, \tag{18}$$

$$S_{es} = 4\pi R_{es}^2 = 4\pi (1 + e_i)^{2/3} R_s^2 = (1 + e_i)^{2/3} S_s, \tag{19}$$

Substitution of Equations (16) and (19) into Equation (15) gives

$$R_H = \frac{V_w}{S_{wl}} = \frac{\delta e_e V_s}{(1 + e_i)^{2/3} S_s} = \frac{1}{A_s \rho_s} \frac{\delta e_e}{(1 + e_i)^{2/3}} \tag{20}$$

The relationship between the effective void ratio and the total void ratio can be established based on the influence of surface area ratio δ on pores. The relationship between the effective void ratio and the total void ratio can be assumed as follows:

$$\frac{V_{im}}{V_m} = an^\delta + b, \tag{21}$$

where a and b are constant parameters that can be calculated according to the boundary conditions, n is porosity.

Two extreme boundary conditions are considered to solve a and b, when the porosity tends to 0 and 1, respectively, then

$$\frac{V_{im}}{V_m} = 1 = a \cdot 0^\delta + b, \tag{22}$$

$$\frac{V_{im}}{V_m} = 0 = a \cdot 1^\delta + b \tag{23}$$

The values of a and b are -1 and 1, respectively. Then, Equation (21) can be expressed as

$$\frac{V_{im}}{V_m} = \frac{e_i}{e} = 1 - n^\delta \tag{24}$$

Then, the effective void ratio and the ineffective void ratio can be computed as

$$e_i = e - \frac{e^{\delta+1}}{(e+1)^\delta}, \tag{25}$$

$$e_e = e - e_i = \frac{e^{\delta+1}}{(e+1)^\delta} \tag{26}$$

Substitution of Equations (20), (25), and (26) into Equation (14) gives

$$k_{\text{sat}} = C_s \frac{g}{\mu A_s^2 G_s^2 \rho_w} \frac{\delta^2 e^{3\delta+3}}{\left[(1+e)^{\delta+1} - e^{\delta+1}\right]^{4/3} (1+e)^{5/3\delta+1}} \tag{27}$$

EVALUATION AND VALIDATION

The improved equation is evaluated using a database comprised of 450 experimental values of k_{sat} and e from 10 publications containing clayey soils, silty soils, and sandy soils (Table 1). The hydraulic conductivity test methods are represented in the database: falling-head test, constant-head test, consolidation test, and oedometer test. Only data for saturated hydraulic conductivity measured with water as the permeant are included. The data plotted in this study include disturbed and undisturbed specimens.

The liquid limit and plasticity index are used for classification of fine-grained soils based on a Plasticity Chart (Figure 5) given in the standard by ASTM (2017). The database consists of 119 lean clays, 193 fat clays, 41 silts, and 71 elastic silts.

The liquid limit and plasticity index are used for the classification of fine-grained soils based on a Plasticity Chart (Figure 5) given in the standard by ASTM (2017). The database consists of 119 lean clays, 193 fat clays, 41 silts, and 71 elastic silts.

Six specimens in the database without providing liquid limit and plastic limit were classified as silty soils in the literature, and there are 20 sandy soils in the database. According to the above classification of fine-grained soils,
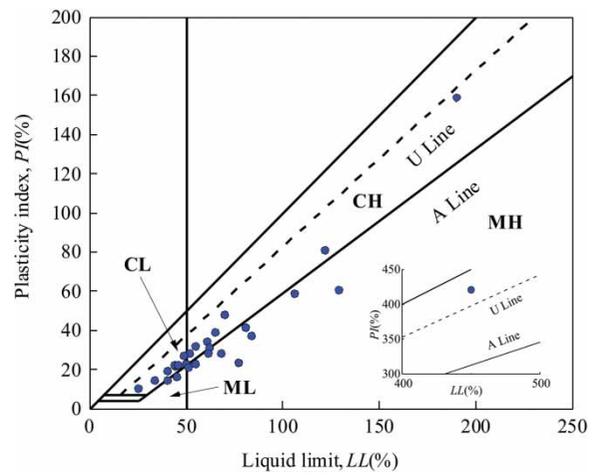

Figure 5 │ Soils plotted on a Plasticity Chart.

Table 1 │ Summary of the database

Sources	Materials	n	Experimental method	Liquid limit	Plastic limit	G_s	USCS
Lambe & Whitman (1969)	Boston silt	6	Laboratory permeability test	/	/	/	Silt
Mesri & Olson (1971b)	Kaolinite, smectite	72	Consolidation test	40–1,160	27–47	2.65–2.8	CH, ML
Tavenas et al. (2011)	Champlain sea clays, Canadian clays	118	Permeability test and oedometer test	20–74	14–28	/	CH, CL
Towhata et al. (1993)	Bentonite	9	Consolidation test	450	29	2.785	CH
Nagaraj et al. (1994)	Red soil, Brown soil, Black cotton soil, Marine soil	72	Falling-head test	50–106	27–47	2.64–2.67	CH, MH
Terzaghi et al. (1996)	Berhierville clay, St. Hilaire clay, Batiscan clay, Vasby clay	113	Falling-head and constant-head test	46–122	22–41	/	CL, CH
Dolinar (2009)	Crystallized kaolinite, Calcium montmorillonite	25	Falling-head test	40.1–129	25.9–68.2	/	ML, MH
Kim et al. (2013)	Marine fine-grained sediments	15	Consolidation test	38.8–77	11.3–27.4	2.45–2.74	MH
Wang et al. (2018)	Calcareous soil	20	Constant-head test	/	/	2.78–2.80	Sand

the database consists of 312 (69.4%) clayey soils, 118 (26.2%) silty soils, and 20 (4.4%) sandy soils.

Simplifying the equation gives

$$C = C_s \frac{g}{\mu A_s^2 G_s^2 \rho_w} \tag{28}$$

Then, Equation (27) can be generalized as

$$k_{sat} = C \frac{\delta^2 e^{3\delta+3}}{[(1+e)^{\delta+1} - e^{\delta+1}]^{4/3}(1+e)^{(5/3)\delta+1}}, \tag{29}$$

Parameters C and δ were obtained by fitting a series of k and e values using nonlinear regression. Then, the hydraulic conductivity was predicted by substituting the fitted parameters C and δ into the proposed equation. It is relatively accurate if a predicted k value of a soil lies between one-third and three times the measured k value, which is within the expected margin of variation for the usual laboratory permeability test results. The predicted values are plotted on a log–log scale against the measured values (Figure 6). The result shows that the accuracies of clayey

soils, silty soils, and sandy soils with two fitted parameters are 94.6, 96.6 and 100%, respectively, while the accuracy of all samples is 95.3%, which means that the improved Kozeny–Carman equation based on the surface area ratio has a satisfactory capability to predict hydraulic conductivity for a wide range from clayey soils to sandy soils.

DETERMINATION OF THE PARAMETERS C AND δ

The empirical or semi-empirical relationships between C and δ and some easily available parameters are established for facilitating the use of the improved equation. The value of parameter C_s, which depends on porosity, microstructures of pores, and capillaries, is not a constant. Due to the lack of available test temperature information from most of the literature, temperature-related parameters such as dynamic viscosity μ_w cannot be accurately evaluated. In summary, the parameter C_s cannot be obtained simply by calculation. Therefore, we studied the correlation between the parameters and the specific surface area of soils.
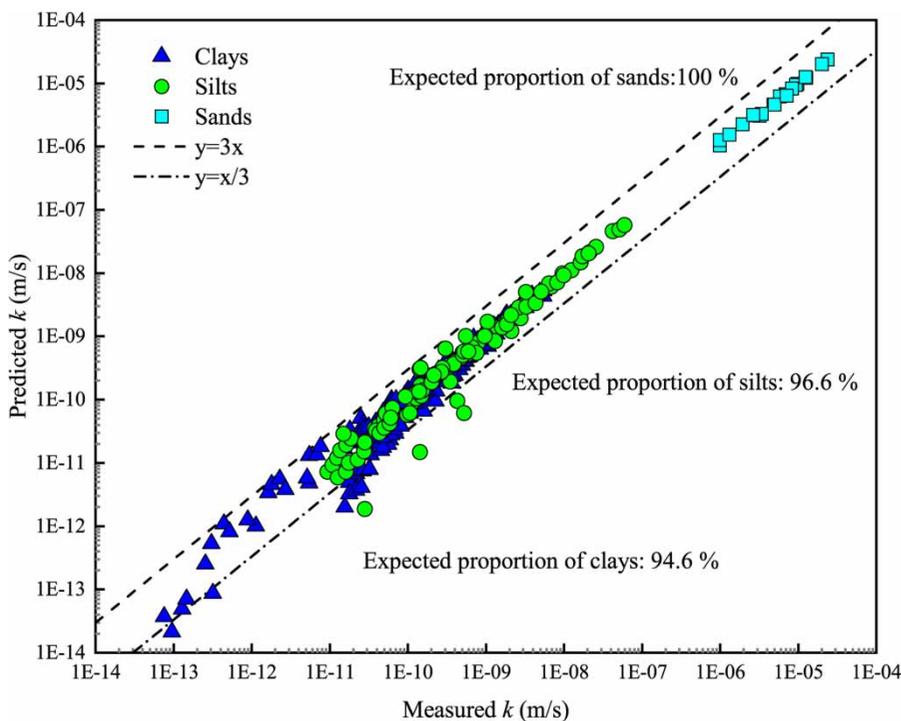
Figure 6 | Predicted k versus measured k values for different soils. Data sources: Lambe & Whitman (1969); Mesri & Olson (1971b); Tavenas *et al.* (2011); Towhata *et al.* (1993); Nagaraj *et al.* (1994); Terzaghi *et al.* (1996); Dolinar (2009); Kim *et al.* (2013); Wang *et al.* (2018).

Various techniques are used to measure the specific surface of solids. The gas adsorption method and the methylene blue absorption method are the most commonly used techniques (Santamarina *et al.* 2002). However, these techniques are not commonly used in soil mechanics and hydrogeology because several of them require the use of high-tech equipment (Chapuis 2012). Alternatively, the specific surface area can be estimated based on complete particle size distribution or empirical relationships with the Atterberg Limit.

The method to determine A_s from the complete particle size distribution is applicable to soils in which particle behaviour is governed by gravimetric-skeletal forces rather than surface-related forces such as nonplastic soils (Sanzeni *et al.* 2013). The specific surface area of sands is a function of particle size and shape (Fair *et al.* 1933). Many later researchers have studied and proposed some formulas for the calculation of the specific surface area of sands (Chapuis & Legare 1992; Carrier 2003).

Santamarina *et al.* (2002) proposed the correlation for estimating the specific surface area of sands made of spherical or cubical particles:

$$A_s = \frac{3(C_u + 7)}{4\rho_w G_s D_{50}},$$

(30)

where C_u is the coefficient of uniformity, and D_{50} is the particle diameter corresponding to 50% passing.

The specific surface area of plastic soils can be estimated empirically based on the plasticity index properties. Numerous studies have shown that A_s of plastic soils is related to the liquid limit, the plastic limit, the shrinkage limit, and the plasticity index (Nishida & Nakagawa 1969; Sridharan & Honne 2005; Farrar & Coleman 2006; Feng & Vardanega 2019; Spagnoli & Shimobe 2019).

Fine-grained soils contain free water in addition to strongly adsorbed water. Then, the total water content can be expressed as

$$w_t = w_{iw} + w_{mw},$$

(31)

where w_t is the total water content, w_{iw} is the adsorbed water content, and w_{mw} is the free water content.

The three primary ways in which clay particles can be arranged are: edge to edge, edge to face, and face to face. Dawson (1975) observed that clay particles become parallel as they shear past each other. Goodeve (1939) proposed

$$F = \frac{fcz}{2},$$

(32)

where F is the shearing force per unit area, f is the critical force required to break an interparticle bond or link, c is the number of bonds or links per unit volume, and z is the distance between two particles.

Two parallel clay particles with length, width, and height of a, b, and c are shown in Figure 7. Then, the volume of the particle is

$$V_s = abc,$$

(33)

and the mass of the particle is

$$Y = \frac{\Delta M_0}{\Delta[\text{isoprene}]}$$

(34)

The specific surface area of particle can be expressed as

$$A_s = \frac{A}{m_s} = \frac{2(ab + bc + ac)}{abc G_s \rho_w}$$

(35)

With the assumption that the thickness of the adsorbed water is t, the adsorbed water content is

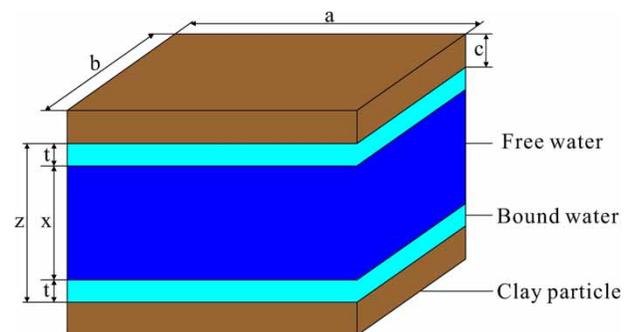$$w_{im} = \frac{[2(a + 2t)(b + 2t)t + 2(b + 2t)ct + 2act]\rho_w}{abc G_s \rho_w}$$

(36)

Figure 7 | Representative unit of parallel clay particles.

The free water content and total water content can be expressed as

$$w_{\mathrm{mw}} = \frac{m_{\mathrm{mw}}}{m_{\mathrm{s}}} = \frac{abx\rho_{\mathrm{w}}}{abc\rho_{\mathrm{s}}} = \frac{x}{cG_{\mathrm{s}}}, \tag{37}$$

$$w_{\mathrm{t}} = w_{\mathrm{iw}} + w_{\mathrm{mw}} = A_{\mathrm{s}}t\rho_{\mathrm{w}} + \frac{4t^2(a+b+c) + 8t^3}{abcG_{\mathrm{s}}} + \frac{x}{cG_{\mathrm{s}}} \tag{38}$$

The parameters t^2 and t^3 tend to 0 because adsorbed water at the corners of the clay particle is negligibly small. Then, Equation (38) is simplified to

$$w_{\mathrm{t}} = A_{\mathrm{s}}t\rho_{\mathrm{w}} + \frac{x}{cG_{\mathrm{s}}} \tag{39}$$

Neglecting the contribution of edges to A_{s}, the specific surface area is

$$A_{\mathrm{s}} = \frac{2ab}{abc\rho_{\mathrm{s}}} = \frac{2}{c\rho_{\mathrm{s}}} \tag{40}$$

By substituting Equation (40) into Equation (39), the results are expressed as

$$z = \frac{2w_{\mathrm{t}}}{A_{\mathrm{s}}\rho_{\mathrm{w}}} = 2\frac{F}{fc}, \tag{41}$$

$$w_{\mathrm{t}} = \frac{F\rho_{\mathrm{w}}}{fc}A_{\mathrm{s}} \tag{42}$$

Equation (42) can be expressed in the form below at the liquid limit:

$$\mathrm{LL} = \frac{F\rho_{\mathrm{w}}}{fc}A_{\mathrm{s}}, \tag{43}$$

where fc is the force required to break all the bonds or links per unit volume. Muhunthan (1991) proposed

$$fc = \beta A_{\mathrm{s}} + \gamma \tag{44}$$

Different fine-grained soils have an approximately equal undrained shear strength at the liquid limit (Casagrande 1932). Hence, F is approximately a constant at the liquid

limit. Equation (44) can be written as follows:

$$\left.\frac{fc}{F\rho_{\mathrm{w}}}\right|_{\mathrm{LL}} = \eta A_{\mathrm{s}} + \lambda, \tag{45}$$

Combining with Equation (45), Equation (43) can be modified as follows:

$$\frac{1}{\mathrm{LL}} = \lambda\frac{1}{A_{\mathrm{s}}} + \eta \tag{46}$$

The results of De Bruyn (1957), Farrar & Coleman (2006), Locat *et al.* (1984), Sridharan *et al.* (1986), Sridharan *et al.* (1988), and Yukselen-Aksoy & Kaya (2010) have been plotted in Figure 8. Linear regression analysis was used to solve for parameters λ and η. The best-fitted line ($R^2 = 0.7054$) of Figure 8 corresponds to the equation as follows:

$$\frac{1}{A_{\mathrm{s}}} = 1.093\frac{1}{\mathrm{LL}} - 0.0045, \tag{47}$$

Figure 9 shows that there is no obvious relationship between δ and the specific surface area that is related to the type of soil. The values of parameter δ for clays, silts, and sands are in the ranges of 1–3, 1–6 and 5–6.5, respectively.
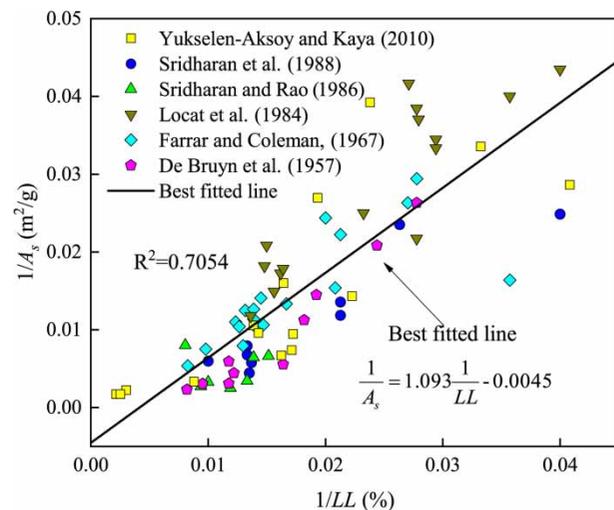
Figure 8 │ Relationship between LL and As. Data sources: De Bruyn (1957); Farrar & Coleman (2006); Locat *et al.* (1984); Sridharan *et al.* (1986); Sridharan *et al.* (1988); Yukselen-Aksoy & Kaya (2010).
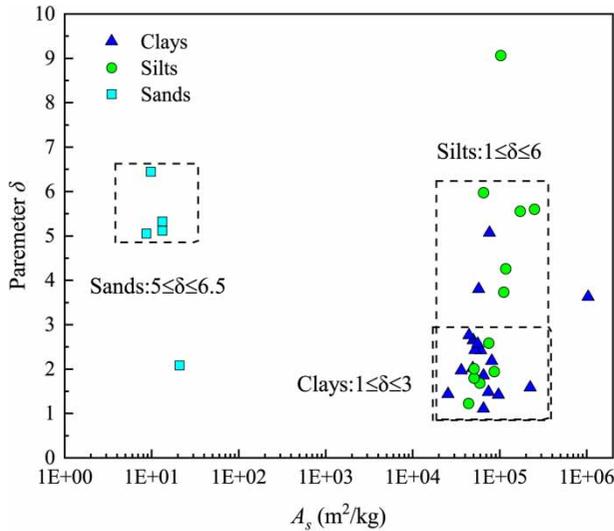
Figure 9 | Relationship between δ and As.

Figure 10 illustrates that there is an approximately linear correlation between parameter C and the specific surface area on a log–log scale. The best-fitted straight line ($R^2 = 0.8429$) is

$$C = 7.66A_{\mathrm{s}}^{-1.8} \tag{48}$$

Following the above analysis, with the assumption that the values of δ are equal to 2, 3, and 5 for clays, silts, and sands, the hydraulic conductivity was computed with one fitted parameter C. The predicted values were plotted on
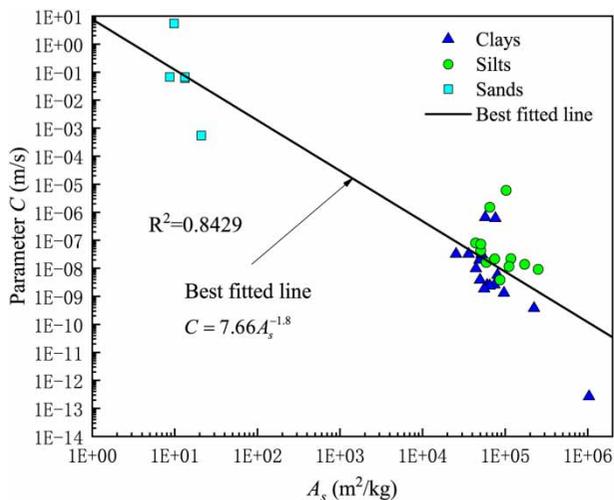

Figure 10 | Relationship between C and As.

a log–log scale against the measured values (Figure 11). The result shows that the accuracies of clayey soils, silty soils, and sandy soils with one fitted parameter are 97.1, 91.5, and 100%, respectively, while the accuracy of all samples is 95.8%. The difference in accuracy between one fitted parameter and two fitted parameters is quite limited. However, values computed with one fitted parameter of silty soils produce a larger error, probably because the value of δ has a wider range of variation causing relatively large scatter.

Figure 12 shows that there is a stronger correlation between the parameter C and the specific surface area with one fitted parameter δ. The best-fitted line ($R^2 = 0.9401$) is

$$C = 11.1A_{\mathrm{s}}^{-1.88}. \tag{49}$$

DISCUSSION

We can consider that the proposed model has a satisfactory capability to predict hydraulic conductivity for a wide range of soils from clays to sands. The deviation of the prediction results may be caused by such factors as input parameters, specimen preparation methods, and unsaturated specimens.

The specimens used in the database include disturbed and undisturbed specimens. The test methods contain the falling-head test, the constant-head test, the consolidation test, and the oedometer test. In addition, the temperatures during the tests are not constant. All the aforementioned factors will give rise to the uncertainty in the true k values. In particular, the compaction method during specimen preparation is critical for the measured values. Heavy compaction should be avoided for the creation of high pore pressure and local internal erosion or clogging, and otherwise large errors of the measured values may result (Chapuis & Aubertin 2003).

The standard for the permeability test (ASTM 2002) indicates that the specimens should be saturated by using a vacuum pump. However, Chapuis (2004) proposed that if a rigid-wall permeameter is used without precautions that are not mandatory in the standard, the degree of saturation is usually in a range of 75–85%. Then, the unsaturated k
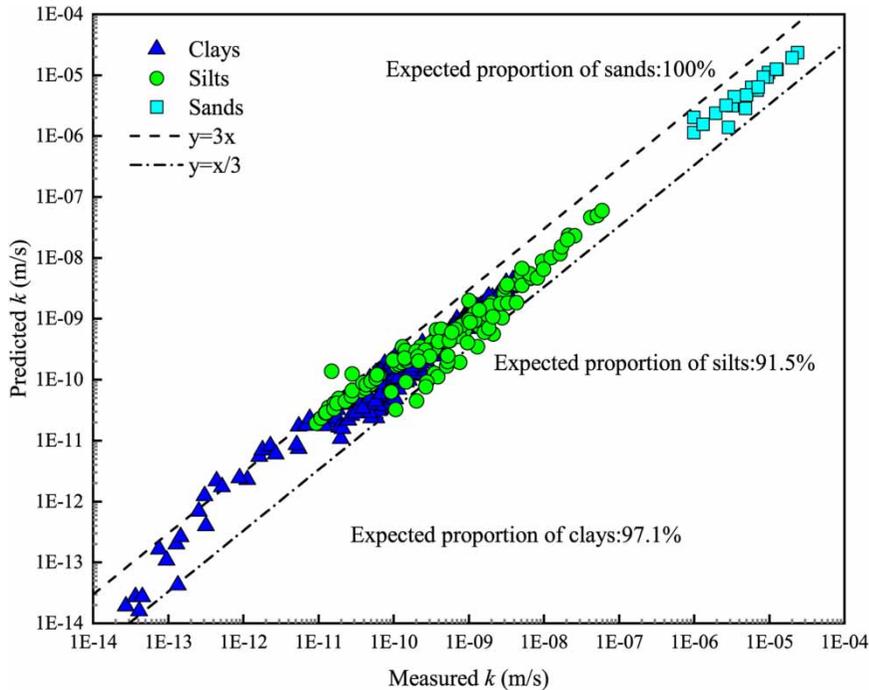
Figure 11 │ Predicted k versus measured k values for different soils after determining the value of δ. Data sources refer to Figure 6.
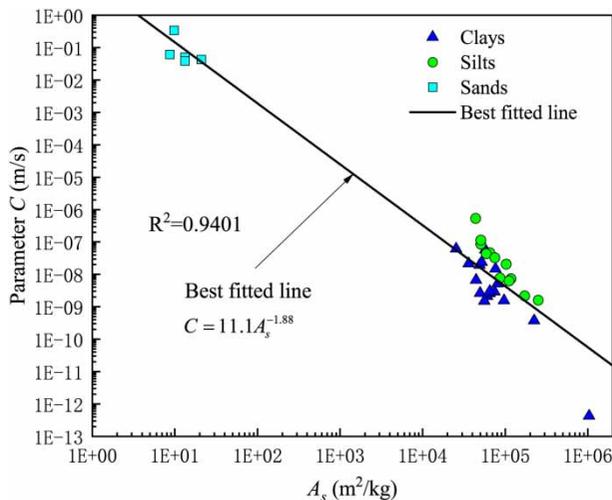
Figure 12 │ Relationship between C and As with one fitted parameter.

value is only 15–30% of the fully saturated k value. In other words, if a specimen is not fully saturated, the true k value may be multiple the measured k value, in which case a large error between k_p and k_m will be induced.

The values of parameter δ also have a definite region for any specific type of soils. For prediction of the hydraulic conductivity, we assumed that the parameter δ is constant, which leads to a larger scatter and inaccuracy. Most previous publications did not provide the information of specific surface area. The value of the specific surface area, which is empirically estimated by the correlation with other available parameters such as liquid limit and the coefficient of uniformity, is the main cause of the inaccuracy of C and the prediction values.

CONCLUSIONS

An improved model of the soil particle-water system is proposed, which presents an explanation for the reduction of the seepage area. A new equation for predicting hydraulic conductivity is derived based on the surface area ratio δ and the total void ratio e. By using published data, the proposed equation is used to predict the vertical k. The results show that the equation provides a good prediction of hydraulic conductivity, ranging mostly within 1/3–3 times for a wide range of soils from clays to sands. The equation can be used for a simple estimate of the vertical k of soils after determining A_s and e and a check on the accuracy of laboratory permeability test results.

The surface area ratio δ is a key parameter for predicting hydraulic conductivity, but it cannot be determined through theoretical derivation. To obtain a more accurate value of the parameter δ, the size, distribution, shape, contact, and other properties of soil particles should be further studied. The anisotropy of hydraulic conductivity is beyond the scope of this paper, because the proposed method uses only scalar parameters such as void ratio and specific surface area to predict the vertical k values. Therefore, the improved equation cannot represent the anisotropy of hydraulic conductivity correctly.

AUTHOR CONTRIBUTIONS

G.X. initiated and led this research. M.W. designed the analytical framework of this study, produced maps and figures, performed the data analysis and interpretation, and wrote the paper. J.W. and Y.Z. contributed the sections. X.K. reviewed and edited the paper.

COMPETING INTERESTS

The authors declare that they have no conflict of interest.

ACKNOWLEDGEMENTS

DATA AVAILABILITY STATEMENT

Data cannot be made publicly available; readers should contact the corresponding author for details.

REFERENCES

Ahuja, L. R., Naney, J. W., Green, R. E. & Nielsen, D. R. 1984 Macroporosity to characterize spatial variability of hydraulic conductivity and effects of land management. *Soil Science Society of America Journal* **48** (4), 699–702.

Alyamani, M. S. & Sen, Z. 1993 Determination of hydraulic conductivity from complete grain-size distribution curves. *Ground Water* **31**, 551–555.

ASTM 2002 *Standard Test Method for Permeability of Granular Soils (constant head) (D2434)*. ASTM International, West Conshohocken, PA.

ASTM 2017 *Standard Practice for Classification of Soils for Engineering Purposes (Unified Soil Classification System) (D2487-17)*. ASTM International, West Conshohocken, PA.

Benson, C. H. & Trast, J. M. 1995 Hydraulic conductivity of thirteen compacted clays. *Clays and Clay Minerals* **43**, 669–681.

Boadu, F. K. 2000 Hydraulic conductivity of soils from grain-size distribution: new models. *Journal of Geotechnical and Geoenvironmental Engineering* **126** (8), 739–746.

Carman, P. C. 1937 Fluid flow through a granular bed. *Transactions of the Institution of Chemical Engineers*. London, 15, pp. 150–156.

Carrier, W. D. 2003 Goodbye, Hazen; Hello, Kozeny-Carman. *Journal of Geotechnical and Geoenvironmental Engineering* **129** (11), 1054–1056.

Casagrande, A. 1932 Research on the Atterberg Limits of soils. *Public Roads* **13**, 121–136.

Chapuis, R. P. 2004 Predicting the saturated hydraulic conductivity of sand and gravel using effective diameter and void ratio. *Canadian Geotechnical Journal* **41** (5), 787–795.

Chapuis, R. P. 2012 Predicting the saturated hydraulic conductivity of soils: a review. *Geology and the Environment* **71** (3), 401–434.

Chapuis, R. P. & Aubertin, M. 2003 On the use of the Kozeny-Carman equation to predict the hydraulic conductivity of soils. *Canadian Geotechnical Journal* **40** (3), 616–628.

Chapuis, R. P. & Legare, P. P. 1992 A simple method for determining the surface-area of fine aggregates and fillers in bituminous mixtures. In: *Effects of Aggregates and Mineral Fillers on Asphalt Mixture Performance*, Vol. 1147 (R. C. Meininger, ed.). American Society for Testing and Materials Special Technical Publication, San Diego, pp. 177–186.

Dawson, R. 1975 An activated-state model for clay suspension rheology. *Journal of Rheology* **19**, 229–244.

De Bruyn, C. 1957 The specific surface, water affinity, and potential expansiveness of clays. *Clay Minerals* **3**, 120–128.

Dolinar, B. 2009 Predicting the hydraulic conductivity of saturated clays using plasticity-value correlations. *Applied Clay Science* **45** (1–2), 90–94.

Dolinar, B. & Trcek, B. 2019 A new relationship between the mobile and the adsorbed water in fine-grained soils using an effective void-ratio estimation. *Bulletin of Engineering Geology and the Environment* **78** (6), 4623–4631.

Dolinar, B., Misic, M. & Trauner, L. 2007 Correlation between surface area and Atterberg limits of fine-grained soils. *Clays and Clay Minerals* **55** (5), 519–523.

Fair, G., Hatch, L. & Jr, H. 1933 Fundamental factors governing the stream-line flow of water through sand. *Journal American Water Works Association* **25**, 1551–1565.

Farrar, D. & Coleman, J. 2006 The correlation of surface area with other properties of nineteen British clay soils. *Journal of Soil Science* **18**, 118–124.

Fauzi, U. 2002 Permeability estimation based on pore radius and its distribution. *Kontribusi Fisika Indonesia* **13**, 2002.

Feng, S. Y. & Vardanega, P. J. 2019 Correlation of the hydraulic conductivity of fine-grained soils with water content ratio using a database. *Environmental Geotechnics* **6** (5), 253–268.

Goodeve, C. 1939 General theory of thixotropy and viscosity. *Transactions of the Faraday Society* **35**, 342–358.

Hansen, D. 2004 Discussion of 'On the use of the Kozeny-Carman equation to predict the hydraulic conductivity of soils'. *Canadian Geotechnical Journal* **41** (5), 990–993.

Hazen, A. 1982 *Some Physical Properties of Sand and Gravel, with Special Reference to Their use in Filtration*. Massachusetts State Board of Health, 24th Annual Report, Boston, pp. 539–556.

Jabro, J. D. 1992 Estimation of saturated hydraulic conductivity of soils from particle-size distribution and bulk-density data. *Transactions of the AsAE* **35** (2), 557–560.

Kango, R., Shankar, V. & Alam, M. A. 2019 Evaluation of hydraulic conductivity based on grain size distribution parameters using power function model. *Water Science and Technology-Water Supply* **19** (2), 596–602.

Kim, H. S., Cho, G. C., Lee, J. Y. & Kim, S. J. 2013 Geotechnical and geophysical properties of deep marine fine-grained sediments recovered during the second Ulleung Basin Gas Hydrate expedition, East Sea, Korea. *Marine and Petroleum Geology* **47**, 56–65.

Koponen, A., Kataja, M. & Timonen, J. 1997 Permeability and effective porosity of porous media. *Physical Review E* **56** (3), 3319–3325.

Kozeny, J. 1927 Uber Kapillare Leitung des Wasser im Boden. *Wien Akad. Wiss* **136**, 271–306.

Lambe, T. W. & Whitman, R. V. 1969 *Soil Mechanics*. John Wiley and Sons, New York.

Locat, J., Lefebvre, G. & Ballivy, G. 1984 Mineralogy, chemistry, and physical-properties interrelationships of some sensitive clays from Eastern Canada. *Canadian Geotechnical Journal* **21** (3), 530–540.

Mesri, G. & Olson, R. 1971a Consolidation characteristics of montmorillonite. *Géotechnique* **21**, 341–352.

Mesri, G. & Olson, R. E. 1971b Mechanisms controlling the permeability of clays. *Clays and Clay Minerals* **19** (3), 151–158.

Muhunthan, B. 1991 Liquid limit and surface-area of clays. *Géotechnique* **41** (1), 135–138.

Nagaraj, T. S., Pandian, N. S. & Raju, P. 1994 Stress-state permeability relations for overconsolidated clays. *Géotechnique* **44** (2), 349–352.

Najafzadeh, M., Laucelli, D. B. & Zahiri, A. 2017 Application of model tree and evolutionary polynomial regression for evaluation of sediment transport in pipes. *KSCE Journal of Civil Engineering* **21** (5), 1956–1963.

Nishida, Y. & Nakagawa, S. 1969 Water permeability and plastic index of soils. *Land Subsidence* **89**, 573–578.

Odong, J. 2007 Evaluation of empirical formulae for determination of hydraulic conductivity based on grain-size analysis. *Journal of American Science* **4** (1) 1–6.

Onur, E. M. & Shakoor, A. 2015 Relationships between grain size distribution indexes and permeability of sands. *Engineering Geology for Society and Territory* **3**, 287–290.

Ren, X. W., Zhao, Y., Deng, Q. L., Kang, J. Y., Li, D. X. & Wang, D. B. 2016 A relation of hydraulic conductivity – void ratio for soils based on Kozeny-Carman equation. *Engineering Geology* **213**, 89–97.

Salarashayeri, A. F. & Siosemarde, M. 2012 Prediction of soil hydraulic conductivity from particle-size distribution. *World Academy of Science, Engineering and Technology* **61**, 454–458.

Santamarina, J. C., Klein, K. A., Wang, Y. H. & Prencke, E. 2002 Specific surface: determination and relevance. *Canadian Geotechnical Journal* **39** (1), 233–241.

Sanzeni, A., Colleselli, F. & Grazioli, D. 2013 Specific surface and hydraulic conductivity of fine-grained soils. *Journal of Geotechnical and Geoenvironmental Engineering* **139** (10), 1828–1832.

Spagnoli, G. & Shimobe, S. 2019 A statistical reappraisal of the relationship between liquid limit and specific surface area, cation exchange capacity and activity of clays. *Journal of Rock Mechanics and Geotechnical Engineering* **11** (4), 874–881.

Sridharan, A. & Honne, N. 2005 Hydraulic conductivity of remolded fine-grained soils versus index properties. *Geotechnical and Geological Engineering* **23**, 43–60.

Sridharan, A., Rao, S. M. & Murthy, N. S. 1986 Liquid limit of montmorillonite soils. *Geotechnical Testing Journal* **9** (3), 156–159.

Sridharan, A., Rao, S. M. & Murthy, N. S. 1988 Liquid limit of kaolinitic soils. *Géotechnique* **38**, 191–198.

Tan, S. A. 1989 A simple automatic falling head permeameter. *Soils and Foundations* **29**, 161–164.

Tavenas, F., Leblond, P., Jean, P. & Leroueil, S. 2011 The permeability of natural soft clays, Part I: methods of laboratory measurement. *Canadian Geotechnical Journal* **20**, 629–644.

Taylor, D. W. 1948 *Fundamentals of Soil Mechanics*. John Wiley and Sons, New York.

Terzaghi, K., Peck, R. B. & Mesri, G. 1996 *Soil Mechanics in Engineering Practice*, 3rd ed. John Wiley and Sons, New York.

Towhata, I., Kuntiwattanaku, P., Seko, I. & Ohishi, K. 1993 Volume change of clays induced by heating as observed in consolidation tests. *Soils and Foundations* **33**, 170–183.

Trani, L. D. O. & Indraratna, B. 2010 The use of particle size distribution by surface area method in predicting the saturated hydraulic conductivity of graded granular soils. *Géotechnique* **60**, 957–962.

Uma, K. O., Egboka, B. C. E. & Onuoha, K. M. 1989 New statistical grain-size method for evaluating the hydraulic

conductivity of sandy aquifers. *Journal of Hydrology* **108** (1–4), 343–366.

Urumović, K. & Urumović Sr., K. 2016 The referential grain size and effective porosity in the Kozeny-Carman model. *Hydrology and Earth System Sciences* **20** (5), 1669–1680.

Wang, X. Z., Wang, X., Chen, J. W., Wang, R., Hu, M. J. & Meng, Q. S. 2018 Experimental study on permeability characteristics of calcareous soil. *Bulletin of Engineering Geology and the Environment* **77** (4), 1753–1762.

Xiao, B. Q., Wang, W., Zhang, X., Long, G. B., Fan, J. T., Chen, H. X. & Deng, L. 2019 A novel fractal solution for permeability and Kozeny-Carman constant of fibrous porous media made up of solid particles and porous fibers. *Powder Technology* **349**, 92–98.

Xu, P. & Yu, B. M. 2008 Developing a new form of permeability and Kozeny-Carman constant for homogeneous porous media by means of fractal geometry. *Advances in Water Resources* **31** (1), 74–81.

Yukselen-Aksoy, Y. & Kaya, A. 2010 Method dependency of relationships between specific surface area and soil physicochemical properties. *Applied Clay Science* **50** (2), 182–190.